## Investigation of pinhole defects in gas diffusion layers for the quality control of proton exchange membrane fuel cells

Yuan, Xiao-Zi; Gu, Elton; Zhao, Nana; Stoll, Jonas; Shi, Zhiqing; Girard, Francois



**Publisher's version / Version de l'éditeur:**
https://doi.org/10.1002/fuce.202300224
*Fuel Cells, 24, 2, pp. 90-99, 2024-04-10*

Received: 6 February 2024 | Revised: 20 March 2024 | Accepted: 25 March 2024

DOI: 10.1002/fuce.202300224

Fuel Cells
From Fundamentals to Systems

RESEARCH ARTICLE

# Investigation of pinhole defects in gas diffusion layers for the quality control of proton exchange membrane fuel cells

**Xiao-Zi Yuan**[1] | **Elton Gu**[1] | **Nana Zhao**[1] | **Jonas Stoll**[2] | **Zhiqing Shi**[1] | **Francois Girard**[1]

[1]Energy, Mining & Environment Research Centre, National Research Council Canada, Vancouver, British Columbia, Canada

[2]Fuel Cell Research Lab (FCReL), School of Mechatronic Systems Engineering, Simon Fraser University, Surrey, British Columbia, Canada

**Correspondence**
Xiao-Zi Yuan, Energy, Mining & Environment Research Centre, National Research Council Canada, 4250 Wesbrook Mall, Vancouver, BC V6T 1W5, Canada.
Email: xiao-zi.yuan@nrc.gc.ca

**Funding information**
National Research Council Canada

**Abstract**

The gas diffusion layer (GDL), one of the essential components of the membrane electrode assembly (MEA), plays an important role in the performance of proton exchange membrane fuel cells. With respect to this essential component and its specifications, this work intends to examine the impact of GDL defects and their effects on cell performance for component quality control. To understand how GDL defect affects its performance and to what level the defect takes effect, ex situ characterization and in situ fuel cell testing are conducted by comparing pristine and defective GDLs. While ex situ GDL properties incorporate measurements of thickness, conductivity, and permeability under compression, in situ investigation mainly involves polarization curve and electrochemical impedance spectroscopy. Among different types of GDL defects, pinholes are targeted in this work. As such, the evaluation focuses on assessing the effects of varying numbers and sizes of pinhole defects under different relative humidities (RHs). Using the state-of-the-art GDLs, an improved cell performance is observed with defective GDLs (evenly distributed 40 pinholes with a diameter of 0.58 mm) under 100% RH. Results also show that the effect of pinhole defects is sensitive to RH, as well as operating current densities.

**KEYWORDS**
defect, gas diffusion layer, PEM fuel cell, pinhole, quality control

## 1 | INTRODUCTION

As the proton exchange membrane (PEM) fuel cell technology is currently being commercialized, research activities have been shifted from component development toward manufacturing concerns, including component quality control (QC) [1, 2]. Detailed functions, structures, and properties of key fuel cell components have been described previously. In particular, the book of attributes established can serve as a valuable resource for facilitating component characterization and the development of QC tools [3].

The gas diffusion layer (GDL), a key component of PEM fuel cells, has a number of functions in a PEM fuel cell, including mechanical support, gas/water transport, heat transfer, and electrical conduction [3, 4]. It not only plays

an important role in cell performance, but also affects cell durability. Currently, the main challenge regarding the GDL development is to reduce material cost, processing cost, and manufacturing cost without compromising its performance. For example, Ballard Power Systems had explored to reduce the manufacturing cost of GDLs with a target of >50% reduction by employing continuous mixing and coating techniques. In particular, they implemented various on-line tools for the process control of crucial parameters [5].

As part of cost reduction, QC of GDLs is another important aspect for the mass production during the fabrication of GDLs. Additionally, during the manufacturing of the membrane electrode assembly (MEA), the properties of GDLs may change or defects may form, and thus affecting the performance of the MEA. Here, defects are defined as variations in physical and chemical properties, which might negatively influence cell performance and/or durability. This definition applies to all main MEA components. Understanding the MEA component defects, including GDLs, is indispensable, in particular to the development of on-line QC strategies.

The defects arising during the fabrication of the GDL or assembly of the MEA can manifest as pinholes, cracks/scratches, thickness variations, unevenness of conductivity, permeability, and diffusivity, and non-homogeneity of surface roughness [6]. GDL defects may not only affect the cell performance via changes of GDL properties related to gas/water transport (e.g., permeability) and electrical conduction (e.g., bulk resistance and contact resistance), but also plays a role in cell durability [7]. Defects in GDL can be described regarding width, length, or area. So far, there is a lack of tools to diagnose the defects [8] and most of the existing methods are destructive and expensive [9]. In this context, great efforts have been made at the National Renewable Energy Laboratory in on-line defect detection, for example, an IR camera has been implemented to identify surface cuts [10], and combined infrared thermography with a reactive-flow-through technique to diagnose defects of catalyst layers (CL) [8].

To date, very few studies correlating GDL defects to overall cell performance have been reported. This has limited the understanding of defects at the beginning-of-life and how they may propagate during PEM fuel cell operation. Using a segmented cell, Reshetenko et al. [11] investigated the GDL defects on cell performance. They observed a decreased performance in the local defective area, resulting from the low compression. Using the segmented cell, Reshetenko et al. [12] also explored the effect of GDL defects on cell performance using highly permeable samples. Results showed that the local performance is increased with highly permeable GDLs. Further, Reshetenko et al. [13, 14] studied the effect of polytetrafluoroethylene (PTFE) defects using GDLs containing different amounts of PTFE. Performance decrease was also observed due to increased mass transfer caused by the changes in the structure and property of GDLs.

Given the limited research on the topic of real GDL defects and their correlation to cell performance, there is a lack of knowledge of GDL defects and how GDL defect affects its properties and thus to what extent these defects affect cell performance. Understanding of component defects is undoubtedly important for component suppliers of the fuel cell industry to provide quality GDLs, to examine that to what extent defects are allowed, and to develop online QC tools. As such, this research is focused on one of the GDL defects, pinholes, using commercial GDLs in an attempt to understand how pinhole defect affects its performance and to what level the defect takes effect.

## 2 | EXPERIMENTAL

### 2.1 | State-of-the-art GDL

In this work, the effect of pinhole defects was studied using the state-of-the-art carbon fiber paper, Sigracet 22 BB. Basic specifications of 22 BB are listed in Table 1 [15]. Pinholes were obtained using needles with different diameters and the pinholes went through all the GDL thicknesses.

### 2.2 | Ex situ characterization

The main ex situ characterization was conducted using an in-house designed four-in-one device [4]. This four-in-one device is designed to measure thickness under compression (TUC), through-plane resistivity under compression (RUC), in-plane permeability (IPP) under compression, and through-plane permeability (TPP) for the GDL QC. For the TUC measurement, the resolution is <0.1 μm by using the high accuracy sensors. The measurement of RUC is achieved using the four-point approach at a constant current (0.5 A in all cases). Regarding the measurement of IPP, a differential pressure (10 kPa) is applied across the torus sample and IPP is determined based on Darcy's Law by measuring the air flow and GDL thickness. Detailed descriptions on this in-house designed device can be found in Yuan et al. [4]. By adding a two-piece adaptor, this equipment can extend to switch from the in-plane mode to through-plane mode, transforming a three-in-one device into a four-in-one apparatus.

TUC/RUC/IPP under compression were measured using a torus sample (inside diameter (ID) = 12 mm; Outside diameter (OD) = 40 mm), whereas TPP was mea-

**TABLE 1** 22 BB specifications.

| Property | 22 BB | Units |
|---|---|---|
| Thickness | 215 ± 20 | μm |
| Areal weight | 70 ± 15 | $gm^{-2}$ |
| Electrical resistivity | <10 | $m\Omega\ cm^2$ |
| Thermal conductivity | 0.30 | $W\ m^{-1}\ K^{-1}$ |
| Bending stiffness (machine direction [MD]/transverse direction [TD]) | 1.5/0.9 | N mm |
| Compressibility | 20 | % (@1 MPa) |
| Water contact angle (MPL) | >130 | ° |
| Tensile strength (MD/TD) | 6.9/4.6 | MPa |
| PTFE | 5 | wt.% |
| MPL | Yes, on one side | – |

Abbreviations: MPL, micro-porous layer; PTFE, polytetrafluoroethylene.

sured using a disk sample with a diameter of 24 mm. In terms of TPP measurement, the compression load is controlled under 2 MPa with a differential pressure of 250 Pa. Note that all the measurements were conducted using at least three parallel samples of each GDL with or without pinhole defects.

The microscopy images were taken using the VHX-7000 Keyence Digital microscope, which consists of the controller (VHX-7000), fully-integrated camera (VHX-7100) with high-resolution microscopic lenses and high-performance camera (VHX-7020).

## 2.3 | In situ test

In situ performance test was carried out using a Scribner cell fixture with an active area of 25 $cm^2$ on a Scribner Compact Fuel Cell Test Station with a built-in impedance capability. Ion power catalyst coated membrane (CCM) with the HP membrane was selected to investigate the effect of GDL defects. The CCM features an overall dimension of 8 × 8 cm with a catalyst loading of 0.3 mg Pt $cm^{-2}$ for both the cathode and anode. The anode GDL remains unchanged during the experiment while the cathode GDL with or without defects is swapped upon needs. Extra care is taken to swap the cathode GDL in the processes of dissembling and re-assembling the cell. Experiments have shown that removing the GDL does not damage the CCM for a short-term test through ocular observation, as well as repeated performance in duplicate tests.

For a fresh CCM, conditioning was conducted before any performance test under a constant current density of 1 A $cm^{-2}$ while maintaining a voltage above 0.5 V for at least 18 h until no further performance improvement. In terms of performance test, the cell was run under 80°C and 100% relative humidity (RH) with a back pressure of 80 kPa (gauge) for both sides unless otherwise stated. The flow rate was controlled constantly at 2 and 5 slpm, respectively, for $H_2$ at the anode and air at the cathode to ensure sufficient gas supplies.

The electrochemical impedance spectroscopy (EIS) measurement was carried out in a galvanostatic mode using the built-in impedance analyzer of the test station. The impedance spectra were swept over a frequency range of 10 kHz–0.1 Hz. The amplitude of the alternative current (AC) perturbation was maintained at 10% of the direct current (DC), including from low current to high current of 1.25, 2.5, 5, 15, 25, and 30 A (corresponding to 0.05, 0.1, 0.2, 0.6, 0.8, and 1.2 A $cm^{-2}$, respectively) in this work.

# 3 | RESULTS AND DISCUSSION

## 3.1 | Ex situ characterization

The effect of pinhole defects on TUC/RUC/IPP was conducted on torus samples. For the effect of pinhole number, 4, 8, and 12 pinholes with a diameter of 0.58 mm were created, evenly distributed in the middle of the annular samples, while in case of the effect of pinhole size (ranging from 0.58–1.25 mm in diameter as listed in Table 2), eight pinholes were generated and evenly distributed in the middle of the annular samples. The results indicate that differences were not observable in terms of thickness, resistivity, and IPP under compression between the pristine and defective GDLs with pinholes within the studied pinhole size and number range.

Therefore, ex situ characterization was then focused on the effect of pinholes on TPP. In terms of effect of pinhole size, five different sizes were explored, from 0.58 mm to 1.25 mm in diameter, as listed in Table 2, with pinhole percentages ranging from 0.2% to 1.1%. As for the effect of the number of pinholes, five different numbers are studied from one to eight pinholes, also listed in Table 2, with

**TABLE 2** Ex situ experimental design for the effect of pinhole defects on through-plane permeability (TPP).

| Pin hole defects | | Defective GDL samples | | | | |
|---|---|---|---|---|---|---|
| | | GDL1 | GDL2 | GDL3 | GDL4 | GDL5 |
| Pinhole size | Diameter (mm) | 0.58 | 0.68 | 0.85 | 1.01 | 1.25 |
| | Area ($mm^2$) | 0.26 | 0.36 | 0.57 | 0.80 | 1.23 |
| | Percentage of pinholes (%) | 0.2 | 0.3 | 0.5 | 0.7 | 1.1 |
| Number of pinholes[a] | No. of pinholes | 1 | 2 | 4 | 6 | 8 |
| | Area ($mm^2$) | 0.26 | 0.53 | 1.07 | 1.59 | 2.11 |
| | Percentage (%) | 0.2 | 0.5 | 0.9 | 1.4 | 1.9 |

Abbreviation: GDL, gas diffusion layer.
[a]Each pinhole had a diameter of 0.58 mm.

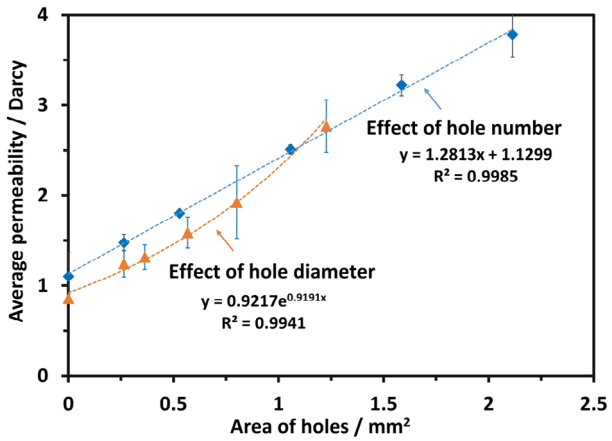


**FIGURE 1** Effect of pinhole defects on through-plane permeability (TPP) under a compression load of 2 MPa and differential pressure of 250 Pa (diamond in blue: TPP as a function of pinhole diameter; triangle in orange: TPP as a function of pinhole number with the pinhole size of 0.58 mm in diameter; and dashed lines are the fitting results). Note: 1 Darcy = $0.986923 \times 10^{-12}$ $m^2$.

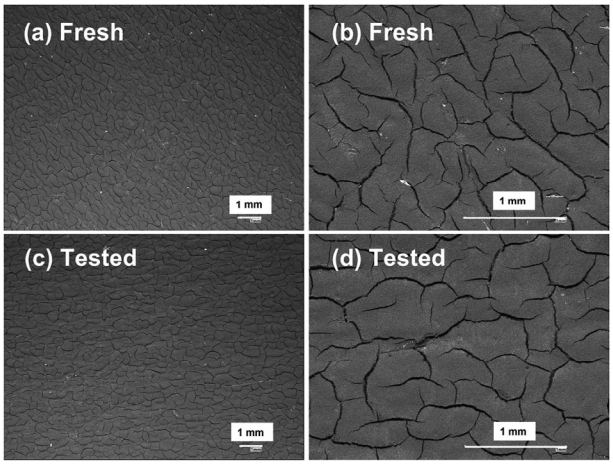


**FIGURE 2** Microscopic images at different magnifications for the micro-porous layer (MPL) side of baseline 22 BB: (a) and (b) before performance test; (c) and (d) after performance test.

pinhole percentages ranging from 0.2% to 1.9%. Results are shown in Figure 1.

As expected, TPP increases with increasing the diameter of pinholes and the increased pattern of TPP is an almost exponential correlation with the pinhole area. Also as expected, TPP increases with increasing the number of pinholes, and a linear relationship is observed between TPP and the area of pinholes. Note that the errors in Figure 1b are lower than those in Figure 1a as the measurements are able to be conducted using the same piece of sample by increasing the number of pinholes for studying the effect of pinhole number, while different samples had to be used for different diameters of pinholes when investigating the effect of pinhole diameter. Repeatability of TPP measurements for different samples and the same sample shows that differences exist between samples (even cut from the same piece of material) and errors could be up to 10%, whereas errors are within 3% for the same sample.

## 3.2 | In situ test

Before comparing the performance of cells with different defective GDLs, each of the cell test, including polarization curve and EIS, was run at least three times. Unless otherwise stated, all the cells were operated under 80°C and 100% RH. Results show that the repeatability of measurements is excellent with the curves overlapping each other among the three runs of each cell, demonstrating that CCM (IonPower), cell assembly and test station are reliable for the investigation.

Figure 2 shows the microscopic images at two different magnifications for the micro-porous layer (MPL) side of baseline 22 BB without pinholes. Clearly, no significant differences in surface characteristics can be observed for the MPL side of fresh and tested GDLs. As a matter of fact, the tested MPL looks cleaner than the pristine MPL, due to the cleaning process (40 cyclic voltammetry cycles at a scan rate of 50 mV $s^{-1}$ between 0.05 and 1.2 V under the $H_2/N_2$ operation mode) operated before MEA conditioning, with less impurity residue. The clean MPL surface in

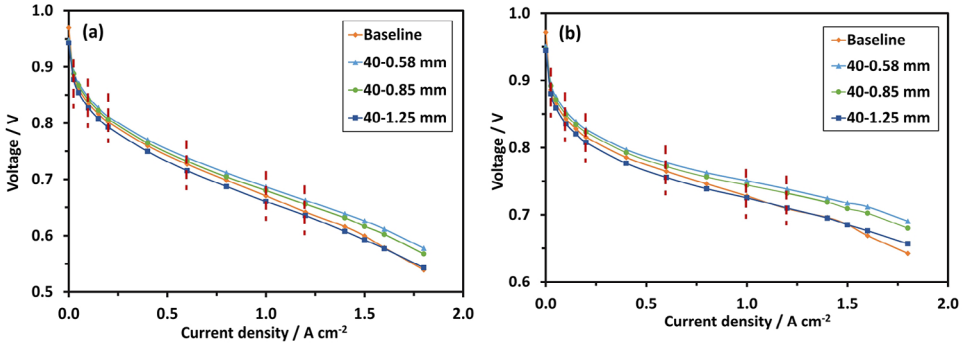


**FIGURE 3** (a) Comparison of cell performance, and (b) comparison of IR-corrected cell performance using gas diffusion layers (GDLs) without (baseline) and with 40 pinholes in different diameters (dashed vertical lines mark where electrochemical impedance spectroscopy (EIS) is measured. Cells were operated under 80°C and 100% relative humidity (RH) with a back pressure of 80 kPa for both sides. The flow rate was controlled constantly at 2 and 5 slpm, respectively, for $H_2$ at the anode and air at the cathode).

Figure 2 after test also demonstrates that "peeling off" the cathode GDL from the tested MEA does not cause noticeable damage on the CL of the cathode side as no detached catalysts were observed on MPL, indicating that changing the cathode GDL only is possible and acceptable for the investigation of GDL defect using the tested CCM. This was also confirmed by the unchanged cell performance after switching to a parallel baseline GDL.

### 3.2.1 | Effect of pinhole size on cell performance

Figure 3a presents the cell performance using GDLs with a total of 40 pinholes (this number was chosen to align with the percentage of hole areas in ex situ test) in different diameters (0.58, 0.85, and 1.25 mm). Figure 3b shows the ohmic drop-corrected (IR-corrected) performance curves using the ohmic resistance measured by current interruption. For comparison, baseline (pristine GDL without pinhole defects) performance is also included in Figure 3a,b. As the curves are close to each other, performance data extracted from Figure 3 at typical current densities are also listed in Table S1 for comparison.

The vertical lines on the polarization curves in Figure 3 are the current points from low to high (1.25, 2.5, 5, 15, 25, and 30 A, corresponding to 0.05, 0.1, 0.2, 0.6, 0.8, and 1.2 A $cm^{-2}$, respectively) where EIS is scanned. Results of EIS measurements at different currents/current densities are presented in Figure 4. The Nyquist plot of the cell consists of one depressed semi-circle for low currents (1.25, 2.5, and 5 A), gradually transitioned to two depressed semi-circles for high currents (25 and 30 A). The low current Nyquist plot can be precisely simulated by an equivalent circuit model (ECM) of Randles cell, shown in the inset of Figure 4a, describing ohmic resistance ($R_{el}$) and the impedance due to the charge transfer process ($R_{ct}$). A Warburg element ($Z_w$) had to be added to the Randles cell to represent the mass transfer process for the high current curves [16, 17], shown in the insets of Figure 4b–d. Constant phase elements are used instead of capacitors due to the porosity and tortuosity characteristics of the electrodes. The tiny component at high frequencies ($C_{HF}$ and $R_{HF}$) for the low current curves is, most likely, related to the electric wiring used for cell connection, which disappears in Figure 4b–d when EIS is measured at increased currents or current densities. This high frequency behavior can be neglected in the discussion since it is not related to the electrode electrochemical processes themselves.

As presented in Figure 3, it is interesting to find that the cell performance improves when GDLs have 40 pinholes with a diameter of 0.58 mm, which is equivalent to eight holes for the anulus sample for ex situ measurements in terms of the percentage of hole areas. This can be explained by the improved charge transfer (Figure 4a) and improved charge transfer and mass transfer (Figure 4b–d) in comparison to the baseline. Improved mass transfer can obviously be ascribed to the increased gas supplies to the CL and fast removal of water due to the macro-through pores in GDLs. Consequently, the increased supplies of reactants and fast removal of water at the interface further facilitate the charge transfer. Note that mass transfer phenomena are not observable for EIS at low current densities. However, with increasing the pinhole size, the performance decreases due to the increased charge transfer resistances at low currents (Figure 4a) and increased mass transfer resistances (Figure 4b–d) at high currents. For the defective GDL (40 × 0.85 mm) cell, the performance is still higher than the baseline. This can be attributed to the slightly smaller charge transfer arc at low currents (Figure 4a), and both decreased charge transfer and mass transfer resistances at high currents (Figure 4c,d) compared to the baseline.

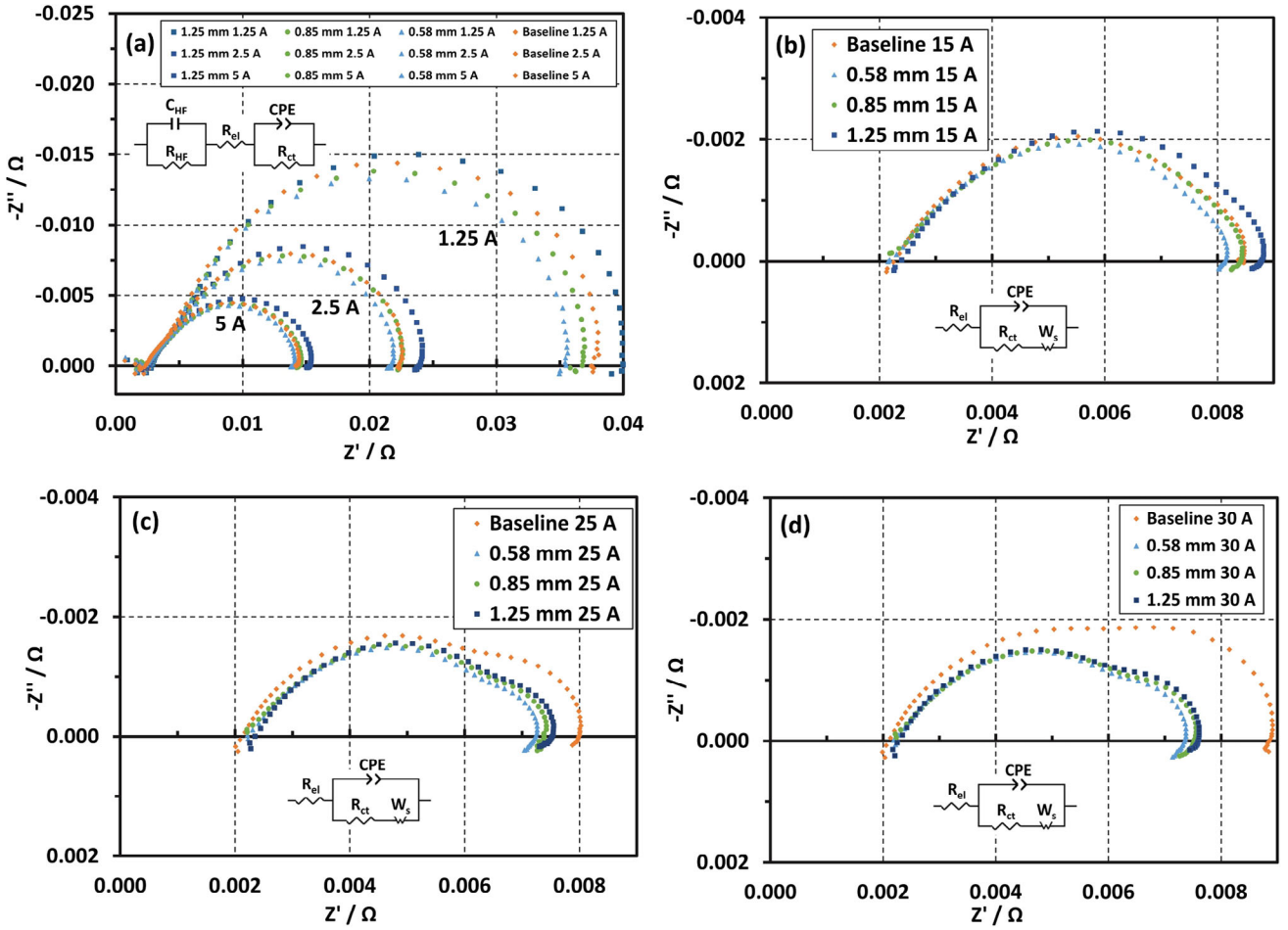


**FIGURE 4** Comparison of Nyquist plots measured at different currents (a) 1.25, 2.5, 5 A; (b) 15 A; (c) 25 A; and (d) 30 A using gas diffusion layer (GDL) with pinhole defect in different diameters.

In general, the results obtained from EIS are consistent with the polarization curves under the operation condition of 80°C and 100% RH, as demonstrated in both Figures 3 and 4. Under the condition of the cell with full hydration, the "defective" pinholes obviously improve mass transfer at high currents within the investigated pinhole size range. Also, the performance trend does not appear to change before and after IR-correction, indicating that pinhole defects in GDLs do not have obvious impact on ohmic resistance.

### 3.2.2 | Effect of the number of pinholes on cell performance

Figure 5 compares the cell performance with and without GDL pinhole defects. Defective GDLs include different numbers of pinholes (10, 40, and 80) with the same diameter of 0.58 mm, corresponding to 0.4, 1.6, and 3.2 holes $cm^{-2}$. Similarly, the vertical lines on the polarization curves in Figure 5 are the current points where EIS is measured. Results of EIS are presented in Figure S1. Again interestingly, we also find that the cell performance improves over the entire current range when GDLs have 40 pinholes with a diameter of 0.58 mm compared with baseline, as seen in Figure 5. This can also be attributed to improved charge transfer at low currents (Figure S1a) and improved charge transfer and mass transfer at high currents (Figure S1b–d) under the operation condition of 80°C and 100% RH. With increasing or decreasing the number of pinholes, the performance of the defective GDLs (10 × 0.85 mm and 80 × 0.85 mm) decreases in comparison to that for the defective GDL (40 × 0.85 mm), however, it is still higher in the high current density range (>0.8 A $cm^{-2}$) compared to the baseline curve, indicating that there is an optimal number (40) of pinholes to better perform with the same diameter of pinholes (0.58 mm). Unexceptionally, the decrease in mass transfer resistance at high currents is obvious in all studied cases with defective GDLs under 100% RH, possibly due to the fast removal of water produced at high operating currents in the presence of pinholes.

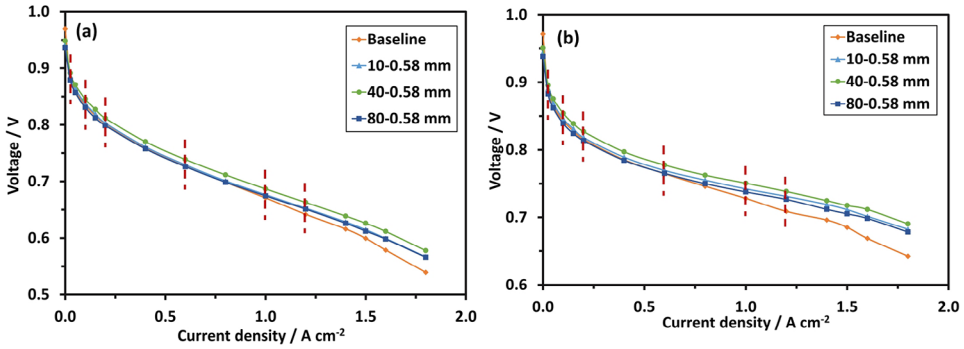


**FIGURE 5** (a) Comparison of cell performance, and (b) comparison of IR-corrected cell performance using gas diffusion layers (GDLs) with/without different numbers of pinholes in a diameter of 0.58 mm (vertical lines mark where electrochemical impedance spectroscopy (EIS) is scanned. Cells were operated under 80°C and 100% relative humidity (RH) with a back pressure of 80 kPa for both sides. The flow rate was controlled constantly at 2 and 5 slpm, respectively, for $H_2$ at the anode and air at the cathode).

In general, it is found that the cell performance for GDLs with defective pinholes (0.58 mm in diameter ranging from 10 to 80 pinholes in this study) is slightly higher than the baseline under 100% RH, especially at high current densities. As the performance difference is small between the curves, voltage data extracted from Figure 5 at typical current densities are also listed in Table S2 for comparison. Under 100% RH, improvement of mass transfer at high current densities is significant. However, there is an optimized number of pinholes (1.6 holes $cm^{-2}$ among the studied scenarios of pinholes in a diameter of 0.58 mm), indicated by the charge transfer resistance at low current densities.

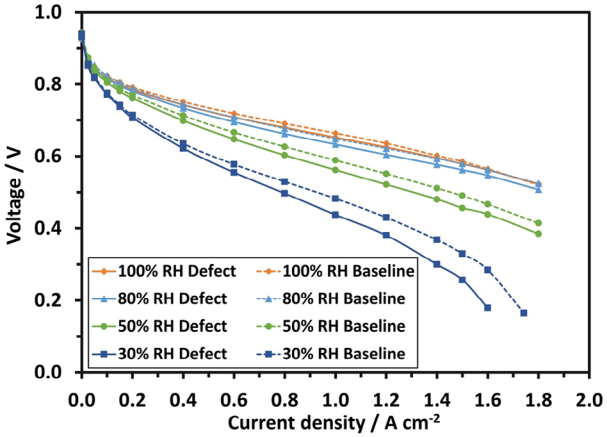


**FIGURE 6** Comparison of baseline cell performance (beginning of test (BOT) baseline) with cell performance using a defective gas diffusion layer (GDL) (40 × 0.58 mm pinholes) under different relative humidities (RHs).

### 3.2.3 | Effect of RH on cell performance

One of the key challenges in the improvement of cell performance is water management within the cell, especially when the cell is performed at high current densities where significant amount of water is produced, resulting in the increase in the oxygen diffusion resistance. Simulations of dynamic two-phase flow have highlighted the significance of pore morphology [18]. In addition to the pore morphology control, hydrophobic coatings, for example, PTFE, have also been used to promote water management within the GDL. Herescu [19, 20] has proved that the defects of coating and the inhomogeneity of coating have direct impacts on water management. On top of the effect of GDL pinhole defect on cell performance, it is of interest to know how GDL pinholes affect water management. As such, the effect of GDL pinholes on cell performance under different RH conditions was investigated in this work. It is worth mentioning that the experiments were run from high RH to low RH using the same MEA in a sequence of baseline GDL, GDL with pinholes, and baseline GDL again. The investigation of GDL with pinholes was conducted on the best performance sample, which is 40 pinholes in a diameter of 0.58 mm.

Figure 6 compares the performance under different RHs for cells with a pristine GDL and GDLs with pinholes. Here, the performance of baselines is under the state of beginning of test (BOT). As seen in Figure 6, for both the baseline sample and sample with pinholes, the performance decreases with decreasing the operating RH. This can be explained by the increase in ohmic (Figure 7a), charge transfer (Figure 7b), and mass transfer resistances (Figure 7c) from low currents to high currents, where Figure 7 presents the fitting results of ohmic, charge transfer, and mass transfer resistances using the ECM shown in Figure 4. Based on the polarization curve, the performance decrease is more obvious when RH is lower than 80%, which is in agreement with previous findings, where the RH increase, usually, enhances the cell performance [21]. Obviously, the lower the RH, the poorer the performance,

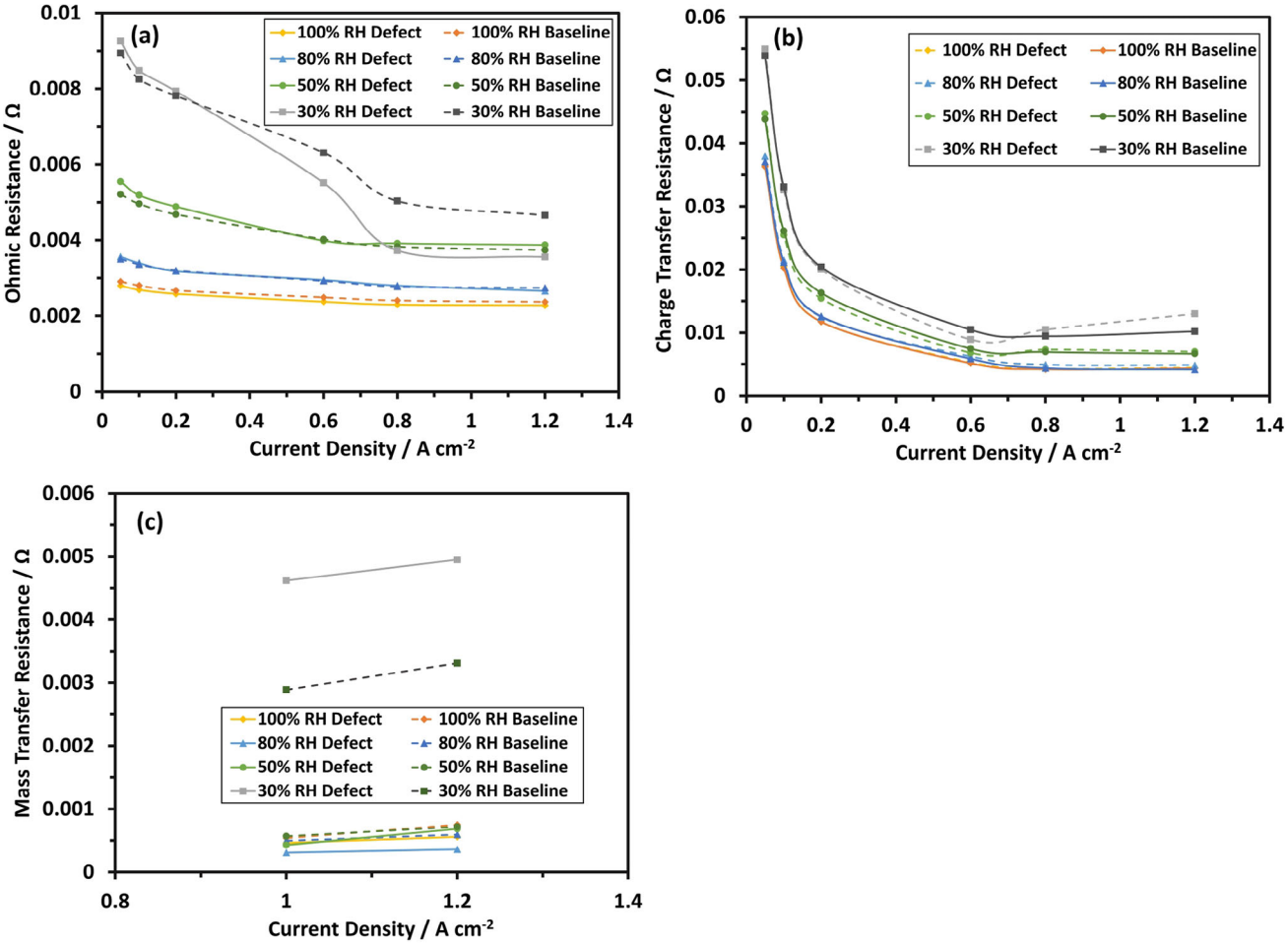


**FIGURE 7** Comparison of end of test (EOT) baseline cell resistances with cell resistances using defective gas diffusion layer (GDL) (40 × 0.58 mm pinholes) under different relative humidity (RH) conditions: (a) ohmic resistance; (b) charge transfer resistance; and (c) mass transfer resistance (data are obtained from electrochemical impedance spectroscopy [EIS] fitting).

and fully hydrated CCM has the best performance without surprise within the studied cases. Under the same RH, the performance of the defective sample is slightly lower than that of the pristine sample at the BOT. The effect is more obvious when RH is lower. However, under 100% RH, this result contradicts with our previous observation in Section 3.3.1, where the cell performance slightly improves when GDLs have 40 pinholes with a diameter of 0.58 mm. The root of this contradiction may come from the test sequence as the GDL sample with pinholes was measured after the baselines from high RH to low RH using the same MEA. It can be explained, possibly, by the MEA degradation caused by the change of RH operation, especially low RH operation at high currents during the measurement of the polarization curves. The change of RH may lead to the membrane expansion or shrinkage, causing mechanical stress and damage of the membrane [22]. In other words, change of RH operation or reduced RH operation (especially 30% RH) greatly accelerates the MEA degradation as negligible differences are observed when the cell is operated under 100% RH even for longer time period. It is concluded that MEA degradation is almost negligible under hydrated normal operation. However, degradation caused by low RH operated, especially extremely low RH (30%) at high current densities, is significant and cannot be neglected.

To really compare the effect of pinhole defect on performance under different RH conditions, performances are compared again using the "end of test (EOT)" baseline (Figure 8) as slight degradation occurred especially after operation under low RH. Note that this "EOT" is not a state after long-term degradation rather than a state after a series test under different RH operations. Similar to what we have observed in Figure 6, with decreasing RH in operation, performance deteriorates for both the baseline sample and the defective sample. Deterioration occurs more significantly when RH is lower. Different from Figure 6, under the same RH, the performance of the sample with pinholes is slightly higher than that of the pristine sample at the EOT in all the studied cases except under

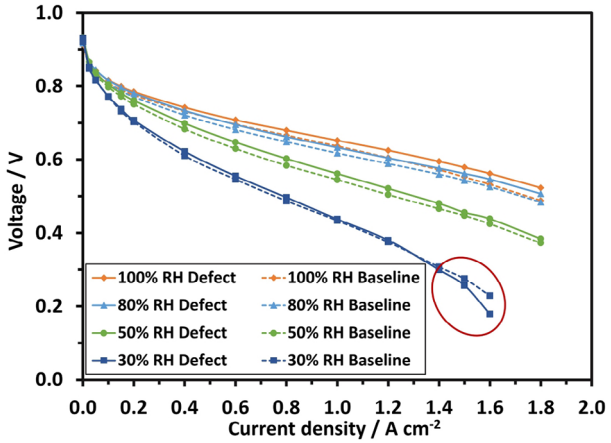


**FIGURE 8** Comparison of baseline cell performance (end of test [EOT] baseline) with cell performance using defective gas diffusion layer (GDL) (40 × 0.58 mm pinholes) under different relative humidities (RHs).

the condition of 30% RH and operated at very high current densities (the circled area in Figure 8). This could be attributed to the facilitation of water management for the pinhole defective GDL with a certain number and size of pinholes unless the MEA is operated under very low RH and high current densities. Nevertheless, for a short-term operation, the difference in performance is not significant for GDLs with and without pinholes. Also, due to the slight difference in performance, no significant difference is observed for EIS curves with and without pinhole defects under the same RH. Unfortunately, this work was not able to complete tests of investigation how defected GDL can perform after long-term operation due to the time-consuming operation.

Studies in literature have demonstrated that structural defects in the GDL can influence cell performance in different aspects [6]: (i) change of water transfer within GDL defects, (ii) change of the electrical contact between components of MEA, and (iii) change of surface features between the MPL and the CL. In case of the pinhole defect, change of surface features and change of the electrical contact are insignificant, and the later has been confirmed based on the RUC test results in this work. Therefore, pinhole defects in the GDL affecting cell performance are possibly dominated by water management, as well as charge and mass transfers in the presence of pinholes, which may affect the transport of reactant gases to the reaction sites, leading to the charge transfer and mass transfer resistances change. All these changes will depend on the RH operating condition, as well as current densities. Therefore, RH plays a key role in the effect of pinhole defects in GDLs and cell performance is highly sensitive to the variations in hydration condition of the cell in operation and operating current densities.

## 4 | CONCLUSIONS

This work examines the customized GDL defects of pinholes on commercial GDLs (22 BB) by measuring properties ex situ and inspecting cell performance in situ with pristine/defective GDLs in an attempt to understand how GDL defect affects its performance.

We find that the effects of pinhole defects on TUC, RUC, and IPP are negligible. As expected, TPP increases with increasing the number and the diameter of pinholes. Interestingly, we also find that the cell performance improves when GDLs have evenly distributed 40 pinholes with a diameter of 0.58 mm (1.6 holes $cm^{-2}$). This can be attributed to an improved charge transfer and mass transfer indicated by the EIS curves under the operation condition of 80°C and 100% RH. Under 100% RH, the improvement of mass transfer is obvious in all studied cases with defective GDLs. The performance of cells using pinhole defective GDLs (0.58 mm in diameter) with a pinhole number ranging from 10 to 80 is slightly higher than that of the baseline cell, especially in the high current density range. However, there is an optimized number of pinholes (40 pinholes with a diameter of 0.58 mm, which is 1.6 holes $cm^{-2}$), indicated by the small charge transfer resistance at low current densities. MEA degradation is almost negligible under fully hydrated normal operation. However, degradation caused by the change of RH, especially when the cell is performed at low RH and high current densities, is significant and cannot be neglected. Cell performance decreases with decreasing the operating RH due to the increased ohmic, charge transfer, and mass transfer resistances and the performance decrease is more obvious when RH is lower than 80%. Under the same RH, minute performance increases are observed for cells with defective GDLs (evenly distributed 40 pinholes with a diameter of 0.58 mm) compared with baselines (EOT) due to the improved mass transfer except under the condition of 30% RH and operated at very high current densities where fast loss of water occurs in the presence of pinholes.

In general, the differences in performance for GDLs with and without pinholes are, likely, minor and not significant although the trend is clear, if the comparison of initial performance is conducted. Long-term operation is needed for considerable gap observation. Also, RH plays a crucial role in the effect of pinhole defects in GDLs and cell performance is highly sensitive to the variations of the operating RH conditions, as well as operating current densities.

## ACKNOWLEDGMENTS

This work is financially supported by the Clean and Energy-Efficient Transportation (CEET) Program of National Research Council Canada (NRC). The authors

appreciate the consultation from the fuel cell industry, in particular, Ballard Power Systems.

Open Access funding provided by the National Research Council Canada library.

## ORCID

*Xiao-Zi Yuan* https://orcid.org/0000-0002-1391-0084

## REFERENCES

1. X.-Z. Yuan, H. Li, E. Gu, W. Qian, F. Girard, Q. Wang, T. Biggs, M. Jaeggle, *World Electr. Veh. J.* **2016**, *8*, 422.
2. X.-Z. Yuan, E. Gu, R. Bredin, M. Baker, S. Lee, T. Biggs, F. Girard, J. Russel, presented at the 30th International Electric Vehicle Symposium, Methods and Devices for Measuring GDL Properties, EVS30, National Research Council Canada, Stuttgart, Baden-Württemberg, Germany, **2017**.
3. X.-Z. Yuan, C. Nayoze-Coynel, N. Shaigan, D. Fisher, N. Zhao, N. Zamel, P. Gazdzicki, M. Ulsh, K. A. Friedrich, F. Girard, U. Groos, *J. Power Sources* **2021**, *491*, 229540.
4. X.-Z. Yuan, E. Gu, R. Bredin, M. Baker, S. Lee, T. Biggs, A. Bock, V. Banhardt, J. Russell, F. Girard, *J. Power Sources* **2020**, *477*, 229009.
5. J. Morgan, Reduction in fabrication costs of gas diffusion layers, *Award Number: DE-FG36-08GO18051, Ballard Material Products, can be found under* https://www.osti.gov/servlets/purl/1045355, **2011**.
6. A. M. Prasad, *Ph.D. Thesis*, University of Waterloo (Waterloo-Ontario, Canada) **2019**.
7. M. Rastedt, F. J. Pinar, P. Wagner, *ECS Trans.* **2014**, *64*, 509.
8. P. K. Das, A. Z. Weber, G. Bender, A. Manak, D. Bittinat, A. M. Herring, M. Ulsh, *J. Power Sources* **2014**, *261*, 401.
9. F. E. Hizir, S. O. Ural, E. C. Kumbur, M. M. Mench, *J. Power Sources* **2010**, *195*, 3463.
10. M. Ulsh, B. Sopori, V. Aieta, N. G. Bender, M. Ulsh, *Electrochem. Soc.* **2012**, *50*, 919.
11. T. V. Reshetenko, G. Bender, K. Bethune, R. Rocheleau, *Electrochim. Acta* **2012**, *80*, 368.
12. T. V. Reshetenko, J. St-Pierre, R. Rocheleau, *J. Power Sources*, **2013**, *241*, 597.
13. T. V. Reshetenko, J. St-Pierre, K. Artyushkova, R. Rocheleau, P. Atanassov, G. Bender, M. Ulsh, *J. Electrochem. Soc.* **2013**, *160*, F1305.
14. T. V. Reshetenko, J. St-Pierre, K. Bethune, R. Rocheleau, *ECS Trans.* **2011**, *41*, 539.
15. Sigracet 22 BB specifications, FuelCell Store, can be found under www.fuelcellstore.com/sigracet-22-bb, **2023**.
16. B. Ghorbani, J. DeVaal, G. Afonso, K. Vijayaraghavan, *Int. J. Hydrog. Energy* **2023**, *48*, 32654.
17. M. Jung, M. D. Ashford, K. A. Williams, *Fuel Cells* **2011**, *11*, 327.
18. D. Niblett, A. Mularczyk, V. Niasar, J. Eller, S. Holmes, *J. Power Sources* **2020**, *471*, 228427.
19. A. Herescu, *ECS Trans.* **2022**, *109*, 77.
20. A. Herescu, *ECS Trans.* **2021**, *104*, 101.
21. K. K. Lai, M. Arif, J. Andrews, S. Cheung, *Int. J. Renew. Energy Res.* **2021**, *11*, 1609.
22. M. Zhang, Y. Liu, Y. Qin, T. Zhang, X. Han, Y. Wang, *Int. J. Green Energy* **2022**, https://doi.org/10.1080/15435075.2022.2155967.

## SUPPORTING INFORMATION

Additional supporting information can be found online in the Supporting Information section at the end of this article.

**How to cite this article:** X.-Z. Yuan, E. Gu, N. Zhao, J. Stoll, Z. Shi, F. Girard, *Fuel Cells* **2024**, *24*, 90. https://doi.org/10.1002/fuce.202300224